International Journal of Engineering Research and Development
e-ISSN : 2278-067X, p-ISSN : 2278-800X, www.ijerd.com
Volume 2, Issue 6 (August 2012), PP. 08-15

Transient Analysis of Continuous Cooling Crystallizers with Needle-Shaped Crystals

Ákos Borsos, Béla G. Lakatos
Department of Process Engineering, University of Pannonia, H8200 Veszprém, 10 Egyetem Street, Hungary

Abstract—Modelling and simulation study of continuous cooling crystallizers is presented for needle-shaped crystals using a detailed two-dimensional population balance model. The population balance equation involves 1D nucleation, growth of two characteristic crystal facets, and is completed with the mass balance equations of solute and solvent, and the heat balances of the crystalline suspension and cooling medium. Simulation has been carried out by using the moment equation model written for the low order joint moments of crystal sizes. The transient behaviour of the crystallizer and the effects of kinetic and process parameters on the characteristics of the crystal size distribution are analysed by simulation.

Keywords—Needle-shaped crystals, Continuous cooling crystallizer, 2D population balance model, Joint moments, Standard moment method, Simulation.

I. INTRODUCTION

Non-isothermal continuous crystallizers, extensively used in the chemical industry, usually are sensitive to both the external and internal disturbances. This is because of the highly nonlinear kinetics, many temperature-dependent parameters, which are, in turn, also nonlinear, and different feedbacks between the variables and elementary processes taking place in crystallization processes. All these properties, as well as the interactions between the kinetics, fluid and heat transfer dynamics as well as the crystal size distribution may give rise to different complexities in both the steady state and dynamic behaviour of continuous crystallizers [1,2].

The crystal size distribution depends on the shape of crystals thus when crystals cannot be described adequately by the often used 1D forms with statistics-based volume shape factors then the influence of shape on the process seems to be important as well. What is more, the shape of crystals produced in solution crystallization usually plays important role in the subsequent applications, especially in the pharmaceutical industry since it influences also the effectiveness of downstream processing significantly.

Needle- or rod-like crystals (crystals with large aspect ratio) are commonly encountered in pharmaceutical and fine chemicals industries thus development of process models [3-9] and of methods for determining the size distribution of crystals [10-14] has received considerable attention. However, detailed population balance model for studying the dynamic aspects of the problem have not been published yet despite that deeper understanding of that seems to be important in relation to both the crystallisation process itself, and to the operation, control, and design of industrial crystallizers with such types of crystals.

The purpose of the paper is to examine the transient characteristics of a continuous cooling crystallizer by developing a 2D population balance model involving 1D nucleation, growth of two characteristic crystal facets, which is completed with the mass balance equations of solute and solvent, and the heat balances of the crystalline suspension and cooling medium. A moment equation model for the joint moments of crystal sizes is determined for simulation purposes. The transient behaviour of the crystallizer and the effects of kinetic and process parameters on the characteristics of the crystal size distribution are analysed by simulation.

II. POPULATION BALANCE MODEL FOR NEEDLE-SHAPED CRYSTALS

A. Population balance equation

Crystals with needle-like habits are simple connected convex polyhedrals and can be characterised by two size dimensions L_1 and L_2, as it is shown in Fig.1, which are sufficient to compute the volumes of crystals, required to develop the mass balance of solute. Namely, in this case the volume of each crystal can be given as

$$v_c(t) = k_V L_1 L_2^2 \quad (1)$$

where k_V is a shape factor referring to the actual form in Fig.1. As a consequence, the crystal population is described by the 2D population density function $(L_1, L_2, t) \rightarrow n(L_1, L_2, t)$ by means of which $n(L_1, L_2, t)dL_1 dL_2$ expresses the number of crystals from the size domain $(L_1, L_1 + dL_1) \times (L_2, L_2 + dL_2)$ in a unit volume of suspension at time *t*.

Let us assume that:

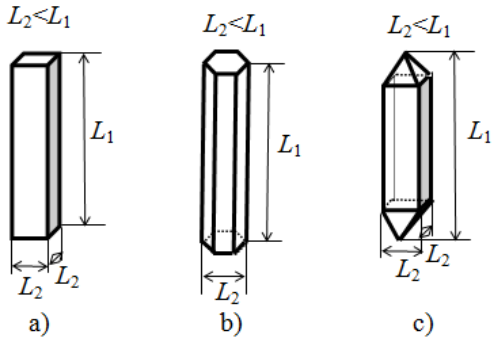

Fig.1 Three different two-dimensional crystal forms

- The crystallizer is perfectly mixed and the working volume is constant.
- The cooling medium can be treated as gradient-less.
- All new crystals are formed at a nominal size $L_{1,n} \cong L_{2,n} \cong L_n \geq 0$, so that we can assume $L_n \approx 0$.
- Crystal breakage and agglomeration are negligible.
- The primary nucleation rate B_p is given by Volmer's model

$$B_p = k_{p0} \exp\left(-\frac{E_p}{RT}\right) \varepsilon \exp\left(-\frac{k_e}{\ln^2\left(\frac{c}{c_s}\right)}\right) \qquad (2)$$

- The rate of secondary nucleation B_b is given by the power law expression

$$B_b = k_{b0} \exp\left(-\frac{E_b}{RT}\right)(c - c_s)^b \upsilon_c^j \qquad (3)$$

- The overall linear growth rates of the two habit faces, G_1 and G_2 are assumed to be size independent and have the forms of power law formulae

$$G_1 = k_{g_{10}} \exp\left(-\frac{E_{g1}}{RT}\right)(c - c_s)^{g_1} \text{ and } G_2 = k_{g_{20}} \exp\left(-\frac{E_{g2}}{RT}\right)(c - c_s)^{g_2} \qquad (4)$$

In Eqs (2) and (4), c and c_s denote, respectively, the solute and equilibrium saturation concentrations, and the kinetic coefficients k_{g10}, k_{g20}, k_{p0} and k_{b0} are constant. In Eq.(3), υ_c denotes the volume of crystal population in a unit volume of suspension, obtained by combining Eq.(1) and the population density function as

$$\upsilon_c = k_V \mu_{1,2}(t) = k_V \int_0^\infty \int_0^\infty L_1 L_2^2 n(L_1, L_2, t) dL_1 dL_2 \qquad (5)$$

while ε in Eq.(2) stands for the volume fraction of solution which is expressed as

$$\varepsilon = 1 - \upsilon_c = 1 - k_V \mu_{1,2}(t) \qquad (6)$$

Under such conditions, the population balance equation takes the form

$$\frac{\partial n(L_1, L_2, t)}{\partial t} + \frac{\partial [G_1 n(L_1, L_2, t)]}{\partial L_1} + \frac{\partial [G_2 n(L_1, L_2, t)]}{\partial L_2} = \frac{1}{\tau}\left[n_{in}(L_1, L_2, t) - n(L_1, L_2, t)\right] \qquad (7)$$

subject to the initial and boundary conditions

$$n(L_1, L_2, t = 0) = n^0(L_1, L_2) \qquad (8)$$

$$\lim_{\substack{L_1 \to 0 \\ L_2 \to 0}} \left[G_1 n(L_1, L_2, t) + G_2 n(L_1, L_2, t)\right] = e_p B_p(L_1, L_2, t) + e_b B_b(L_1, L_2, t) \qquad (9)$$

$$\lim_{\substack{L_1 \to \infty \\ L_2 \to \infty}} n(L_1, L_2, t) = 0 \qquad (10)$$

In Eq.(7), τ stands for the mean residence time while in Eq.(9) e_p and e_b are binary existence variables by means of which the combination of the primary and secondary nucleation rates B_p and B_b can be provided.

B. Mass and heat balance equations

The mass and heat balances are written, respectively, for the solute and solvent, the crystalline suspension and the cooling medium.

The mass balance equation for solute:

$$\frac{dc}{dt} = \frac{\varepsilon_{in}}{\tau\varepsilon}(c_{in} - c) - \frac{\rho_c - c}{\varepsilon} R_{vc} \qquad (11)$$

where R_{vc} denotes the production rate of volume of the crystalline phase referred to a unit volume of suspension, given as

$$R_{vc} = \frac{d\upsilon_c}{dt} \qquad (12)$$

Similarly, the balance equation for the solvent takes the form

$$\frac{dc_{sv}}{dt} = \frac{\varepsilon_{in}}{\tau\varepsilon}\left(c_{sv,in} - c_{sv}\right) + \frac{c_{sv}}{\varepsilon} R_{vc}\,. \qquad (13)$$

The energy balance equation for the crystal suspension is

$$\frac{dT}{dt} = \frac{q}{V}\frac{\phi_{in}}{\phi}(T_{in} - T) - \frac{Ua_V}{\phi}(T - T_h) + \frac{\left(-\Delta H_c\right)}{\phi}\rho_c R_{vc} \qquad (14)$$

where $\varphi = \varepsilon(C_{sv}c_{sv} + C_c c) + (1-\varepsilon)C_c\rho_c$ and $\varphi_{in} = \varepsilon_{in}(C_c c_{in} + C_{sv}c_{svin}) + (1-\varepsilon_{in})C_c\rho_c$.

Finally, the energy balance for the cooling medium is written as

$$\frac{dT_h}{dt} = \frac{q_h}{V_h}(T_{hin} - T_h) + \frac{Ua_V V}{C_h\rho_h V_h}(T - T_h)\,. \qquad (15)$$

The dependence of the equilibrium saturation concentration on the temperature is described by a second order polynomial

$$c_s(T) = a_0 + a_1 T + a_2 T^2 \qquad (16)$$

The set of ordinary equations (11)-(14) are completed with appropriate initial equations.

III. MOMENT EQUATIONS MODEL

The total volume of crystal population in the suspension, required writing the mass balance, and also the heat balance equations can be expressed by means of the joint moment $\mu_{1,2}$ of crystal sizes L_1 and L_2. As a consequence, variation in time of the moment $\mu_{1,2}$ has to be tracked during the course of the process. This can be done by solving the population balance equation (7) using some numerical method, or by developing a set of moment equations for the joint moments

$$\mu_{k,m}(t) = \int_0^\infty\int_0^\infty L_1^k L_2^m n(L_1, L_2, t)\,dL_1 dL_2, \quad k, m = 0,1,2... \qquad (17)$$

required to compute the moment $\mu_{1,2}$ directly. In the later case, the infinite hierarchy of the moment equations corresponding to Eq.(7) becomes of the form

$$\frac{d\mu_{0,0}}{dt} = \frac{1}{\tau}\left(\mu_{0,0,in} - \mu_{0,0}\right) + e_p B_p + e_b B_b \qquad (18)$$

$$\frac{d\mu_{k,m}}{dt} = \frac{1}{\tau}\left(\mu_{k,m,in} - \mu_{k,m}\right) + kG_1\mu_{k-1,m} + mG_2\mu_{k,m-1},\ k+m>0,\ k,m = 0,1,2,3... \qquad (19)$$

This infinite set of equations can be closed at any order but natural closing can be made at the third order joint moment $\mu_{1,2}$ since, because of Eqs (5) and (12), this moment is required for all balance equations (11)-(14) to close. To compute this moment the sequence of equations for moments $\mu_{0,0}, \mu_{1,0}, \mu_{0,1}, \mu_{0,2}, \mu_{1,1}$ are also required:

$$\frac{d\mu_{0,0}}{dt} = \frac{1}{\tau}\left(\mu_{0,0,in} - \mu_{0,0}\right) + e_p B_p + e_b B_b \qquad (20)$$

$$\frac{d\mu_{1,0}}{dt} = \frac{1}{\tau}\left(\mu_{1,0,in} - \mu_{1,0}\right) + G_1\mu_{0,0} \qquad (21)$$

$$\frac{d\mu_{0,1}}{dt} = \frac{1}{\tau}\left(\mu_{0,1,in} - \mu_{0,1}\right) + G_2\mu_{0,0} \qquad (22)$$

$$\frac{d\mu_{1,1}}{dt} = \frac{1}{\tau}\left(\mu_{1,1,in} - \mu_{1,1}\right) + G_1\mu_{0,1} + G_2\mu_{1,0} \qquad (23)$$

$$\frac{d\mu_{0,2}}{dt} = \frac{1}{\tau}\left(\mu_{0,2,in} - \mu_{0,2}\right) + 2G_2\mu_{0,1} \qquad (24)$$

$$\frac{d\mu_{1,2}}{dt} = \frac{1}{\tau}\left(\mu_{1,2,in} - \mu_{1,2}\right) + G_1\mu_{0,2} + 2G_2\mu_{1,1} \qquad (25)$$

Taking into consideration the kinetic rate equations, the set of moment equations (20)-(25) completed with the balance equations (11)-(15) provide a close moment equations model.

IV. SIMULATION RESULTS AND DISCUSSION

The set of 10 ordinary differential equations governing the time evolution of variables $\mu_{0,0}, \mu_{1,0}, \mu_{0,1}, \mu_{0,2}, \mu_{1,1}, \mu_{1,2}, c, c_{sv}, T, T_h$ was solved in MatLab environment using ODE solvers. The basic values of process parameters used in simulation are listed in the Table 1, while the basic values of kinetic parameters of nucleation and crystal growth, as well as of coefficients of the equilibrium saturation concentration used in simulation are shown in Table 2.

TABLE 1: BASIC VALUES OF PROCESS PARAMETERS USED IN SIMULATION

V=10 m^3	τ=10^3 s τ_h=6·10^2 s	Ua_V=5.0·10^5 J kg K^{-1} m^{-3} s^{-1}
T_{in}=90 °C	T_{hin}=18 °C	φ_{in}=3.0·10^6 J kg K^{-1} m^{-3}

TABLE 2 : BASIC VALUES OF KINETIC PARAMETERS USED IN SIMULATION

k_{b0}=2.0·10^7 #/[m^{3}s(kg m^{-3})^b]	k_{p0}=1.6·10^{18} # m^{-3}s^{-1}	a_1=-9.77e-5 kg m^{-3}
k_{g2}=12.2·10^{-6} m/[s(kg m^{-3})^g]	k_{g1}=1.0·10^{-4} m/[s(kg m^{-3})^g]	a_0=0.21 kg m^{-3} K^{-1}
b=2.0. j=1.5 g_1=1.5, g_2=1.75	k_e=0.2 ΔH_c=-44.5 J kg^{-1}	a_2=9.31e-5 kg m^{-3} K^{-2}
E_b=1.5·10^4 J mol^{-1}	E_g=3·10^4 J mol^{-1}	E_p=1·10^4 J mol^{-1}

Fig.2 presents the temporal evolutions of temperatures of the cooling medium and crystalline suspension in answer of the step-wise cooling rate depending on the inlet temperature of the cooling medium. Naturally, the results, especially the transient processes depend also on the cooling strategy but for the sake of obtaining real comparisons of the effects all simulation runs have been performed using such step-wise cooling process strategy with natural cooling process of the crystallizer. Fig.3 presents also the evolutions of these characteristic temperatures but under the influence of variable volumetric flow rate of the

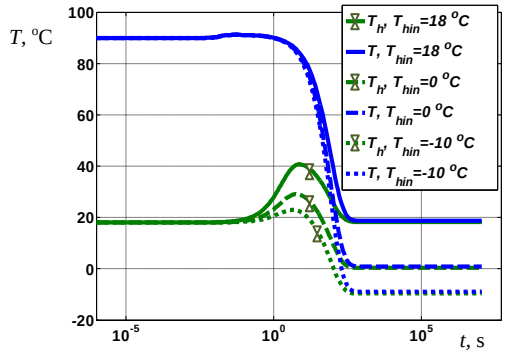

Fig. 2 Evolution of the temperatures of crystalline suspension and cooling medium depending on the inlet cooling medium temperature in the case primary nucleation

cooling medium. In this case the inlet temperature of the cooling medium was 18 ^{O}C. These experiments have shown that under the given process conditions both factors play important role in controlling the crystallizer but the temperature of the cooling medium is the dominant one hence the effects of this factor have been studied more widely.

Figs 4 and 5 demonstrate well that the transient behaviour of the number of crystals, i.e. of the zero order joint moments μ_{00} exhibit characteristic differences. In the case of secondary nucleation when only seed crystals induce production of new crystals the processes appear to be rather smooth, and the steady sate values, i.e. the final crystal numbers are proportional to the inlet temperature of the cooling medium. When, however, primary nucleation occurs in the crystallizer the transient processes usually exhibit large impulses or even damped oscillations as it is shown in Fi.5 for temperatures 18 ^{O}C and 10 ^{O}C. The response for temperature -10 ^{O}C exhibits an interesting feature: the steady state value becomes smaller than that for temperature 0.0 ^{O}C. Since here even the impulse has turned out much smaller it proves that in this case the inertia of the cooling medium-crystallizer system practically filtered out the effects of the quick step-wise temperature input between 18 ^{O}C and -18 ^{O}C.

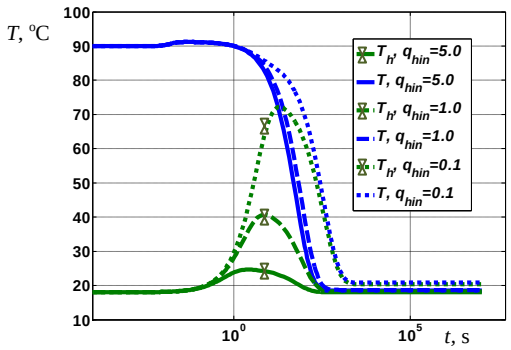

Fig. 3 Evolution of the temperatures of crystalline suspension and cooling medium depending on the volumetric flow rate of cooling medium in the case primary nucleation

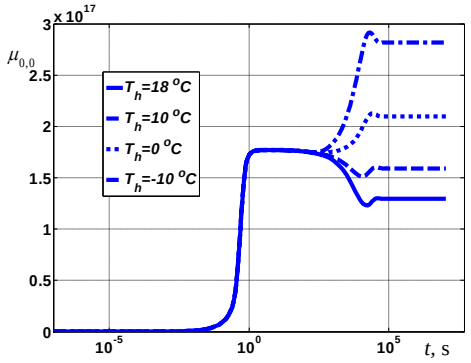

Fig. 4 Evolution of the number of crystals depending on the inlet temperature of cooling medium in the case secondary nucleation

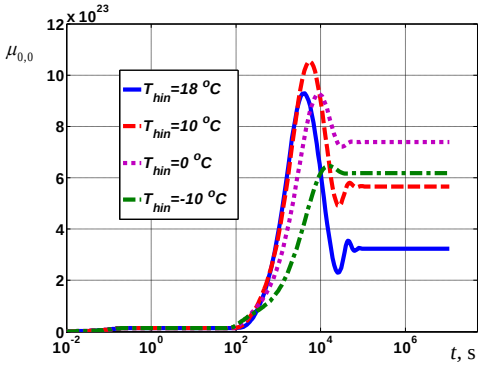

Fig. 5 Evolution of the number of crystals depending on the inlet temperature of cooling medium in the case primary nucleation

Figs 6 and 7 present, respectively, the temporal evolutions of the mean crystal sizes $\langle L_1 \rangle$ and $\langle L_2 \rangle$, defined as $\langle L_1 \rangle = \mu_{1,0}/\mu_{0,0}$ and $\langle L_2 \rangle = \mu_{01}/\mu_{0,0}$ as a function of the inlet temperature of cooling medium in the case of primary and secondary nucleation. Again, characteristic differences between both the transient and stead states are seen showing that the results obtained when secondary nucleation is the dominant generator of the newly born crystals appear to be more scattered. For the sake of comparison, evolutions of the mean crystal sizes $\langle L_1 \rangle$ and $\langle L_2 \rangle$ are presented in Fig.8 in the case if both nucleation mechanisms play important role in affecting the crystal size distribution. Note that the complex transient behaviour of the mean crystal sizes is a consequence of the complex behaviour of the corresponding joint moments. Fig.8 illustrates well

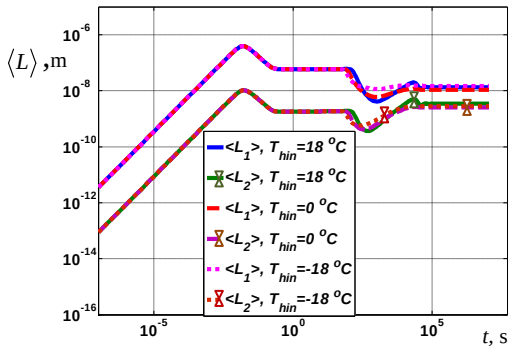

Fig. 6 Evolution of the mean crystal sizes $\langle L_1 \rangle$ and $\langle L_2 \rangle$ depending on the inlet temperature of cooling medium in the case primary nucleation

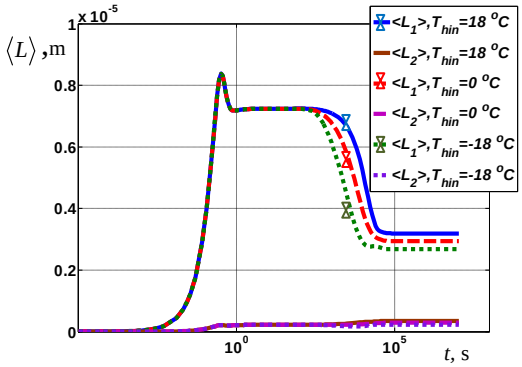

Fig. 7 Mean crystal sizes $\langle L_1 \rangle$ and $\langle L_2 \rangle$ depending on the inlet temperature of cooling medium in the case secondary nucleation

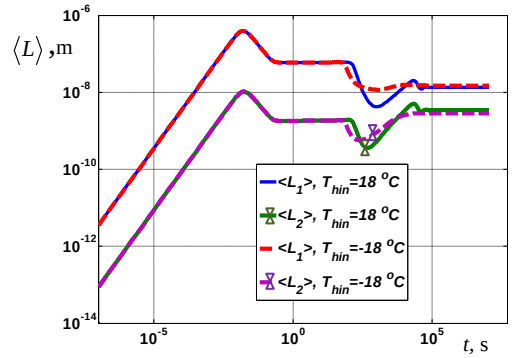

Fig. 8 Mean crystal sizes $\langle L_1 \rangle$ and $\langle L_2 \rangle$ depending on the inlet temperature of cooling medium in the case primary and secondary nucleation

that, although some differences can be observed in the corresponding crystal sizes but the primary nucleation dominates the process definitely.

Figs 9 and 10 show, respectively, the steady state values of the mean crystal sizes $\langle L_1 \rangle$ and $\langle L_2 \rangle$ for primary and secondary nucleation as functions of the corresponding kinetic parameters k_e and b. As is is seen in the regions of small values of parameters k_e and b the differences between the mean crystal sizes obtained for the inlet temperatures 18 ^{o}C and -18 ^{o}C are decreasing monotonously what is more they become of opposite sign. These figures illustrate also that the steady state values of the mean crystal sizes are more scattered in the case of secondary nucleation.

The temporal evolution of the mean aspect ratio defined as $\langle L_1 \rangle / \langle L_2 \rangle$ is presented in Fig.11 for both the primary and secondary nucleation as a function of the inlet temperature of cooling medium. These diagrams reveal that lower cooling temperature results in higher mean aspect ratio in both cases.

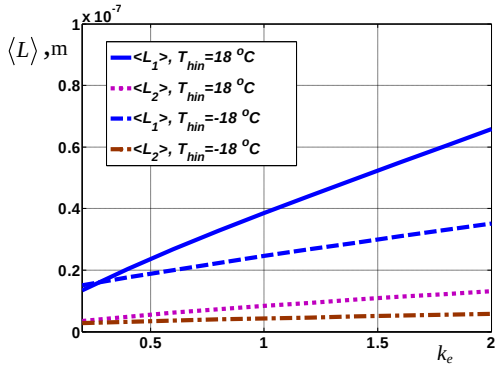

Fig. 9 Mean crystal sizes $\langle L_1 \rangle$ and $\langle L_2 \rangle$ depending on the inlet temperature of cooling medium in the case of primary nucleation

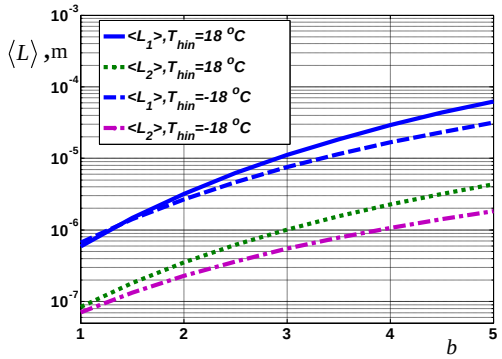

Fig. 10 Mean crystal sizes $\langle L_1 \rangle$ and $\langle L_2 \rangle$ depending on the inlet temperature of cooling medium in the case of secondary nucleation

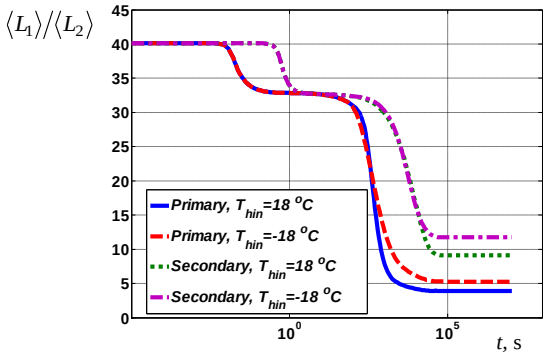

Fig. 11 Evolution of the mean aspect ratio of crystals $\langle L_1 \rangle / \langle L_2 \rangle$ depending on the inlet temperature of cooling medium in the case primary and secondary nucleation

V. CONCLUSIONS

The detailed 2D population balance model which involves a 2D population balance equation as well as the mass balance equations of solute and solvent, and the heat balances of the crystalline suspension and cooling medium has proved a useful tool to study the transient and steady state behaviour of continuous cooling crystallizers with needle-shaped crystals. The moment equations model for the joint moments of crystal sizes can be closed at any order therefore it provides correct results in numerical experimentation.

The transient behaviour of the law order joint moments and, as a consequence, the mean crystal sizes has proved to be rather complex and exhibited characteristic properties depending on the intensity of cooling and the dominant mechanism of nucleation. Analysing the results obtained by simulation allows suggesting that the transient processes measured in situ in crystallizers provide great possibilities to apply in identification of parameters of crystallization.

VI. ACKNOWLEDGMENTS

This work was supported by the TAMOP-4.2.1/B-09/1/KONV-2010-0003 project which is gratefully acknowledged. The financial support by the Hungarian Scientific Research Fund under Grant K77955 is also acknowledged.

SYMBOLS USED

b	exponent of secondary nucleation rate
B	nucleation rate # $m^{-3}s^{-1}$
c	concentration of solute, kgm^{-3}
c_s	equilibrium saturation concentration, kg m^{-3}
C	heat capacity, J K^{-1}
E	activation energy, J mol^{-1}
g	exponent of crystal growth rate
G	crystal growth rate, ms^{-1}
j	exponent of secondary nucleation rate
k_e	parameter of primary nucleation rate
k_g	rate coefficient of crystal growth, $m/[s(kg\ m^{-3})^g]$
k_p	rate coefficient of primary nucleation, # $m^{-3}s^{-1}$
k_b	rate coefficient of secondary nucleation, $\#/[m^3s(kg\ m^{-3})^b]$
k_V	volume shape factor
L	linear size of crystals, m
n	population density function, # m^{-4}
S	supersaturation ratio, c/c_s
T	temperature, °C, °K
υ_c	volume of crystals, $m^3\ m^{-3}$

Greek letters:

ε	volume ratio of solution
$\mu_{k,m}$	$(k,m)^{th}$ order joint moment
ρ	density, kgm^{-3}
τ	mean residence time, s

Subscripts

0	initial value
1	length coordinate of crystals
2	width coordinate of crystals
in	inlet
p	primary nucleation
b	secondary nucleation
h	cooling medium

REFERENCES

[1]. B.G. Lakatos and N. Moldoványi, "Stability and bifurcation of continuous cooling crystallizers," *Hung. J. Ind. Chem.,* vol. 33 pp**.** 49-65, 2005.

[2]. Q. Yin, Y. Song, J. Wang, „Analyses of stability and dynamic patterns of a continuous crystallizer with a size-dependent crystal growth rate," *Ind. Eng.Chem. Res., vol*.42, pp. 630-635, 2003.

[3]. F. Puel, P. Marchal, J. Klein, "Habit transients analysis in industrial crystallization using two dimensional crystal sizing technique," *Trans. IChemE,* vol. 75 (A), pp. 193-205, 1997.

[4]. D.L. M., D.K. Tafti, R.D. Braatz, "High-resolution simulation of multidimensional crystal growth," *Ind. Eng. Chem. Res.,* vol. 41, pp- 6217–6223, 2002.

[5]. F. Puel, G., Févotte, J.P. Klein, "Simulation and analysis of industrial crystallization processes through multidimensional population balance equations. Part 1: a resolution algorithm based on the method of classes," *Chem. Eng. Sci.,* vol. 58, pp. 3715–3727, 2003.

[6]. H. Briesen, "Simulation of crystal size and shape by means of a reduced two-dimensional population balance model," *Chem. Eng. Sci.,* vol. 61, pp. 104-112, 2006.

[7]. K. Sato, H, Nagai, K. Hasegawa, K. Tomori, K., H.J.M. Kramer, P.J. Jansens, "Two-dimensional population balance model with breakage of high aspect ratio crystals for batch crystallization," *Chem. Eng. Sci.*, vol. 63, pp. 3271-3278, 2008.

[8]. S. Qamar, A. Seidel-Morgenstern, "An efficient numerical technique for solving multi-dimensional batch crystallization models with size independent growth rates," Comp. Chem. Eng., vol. 33, pp. 1221-1226, 2009.

[9]. Z. Grof, C.M. Schoellhammer, P. Rajniak, F. Stepanek, "Computational and experimental investigation of needle-shaped crystal breakage," Int. J. Pharmaceutics, vol. 407, pp. 12–20, 2011.

[10]. S. Schorsch, T. Vetter, M. Mazzotti, "Measuring multidimensional particle size distributions during crystallization," *Chem. Eng. Sci.* (2011), doi:10.1016/j.ces.2011.11.029

[11]. C.Y. Ma, X.Z. Wang, K.J. Roberts, „Multi-dimensional population balance modeling of the growth of rod-like L-glutamic acid crystals using growth

[12]. rates estimated from in-process imaging," *Adv. Powder Techn*., vol. 18, pp. 707–723, 2007.

[13]. M. Kempkes, T. Vetter, M. Mazzotti, „Monitoring the particle size and shape in the crystallization of paracetamol from water,", *Chem. Eng. Res. Des*. vol. 88, pp. 447-454, 2010.

[14]. C.Y. Ma, X.Z. Wang, „Closed-loop control of crystal shape in cooling crystallization of l-glutamic acid,", *J. Process Control*, vol. 22, pp. 72–81, 2012.